Materials Transactions, JIM, Vol. 31, No. 12 (1990), pp. 1078 to 1084

Thermodynamics of $Y_2Cu_2O_5$ and $YCuO_2$ and Phase Equilibria in the Ba-Y-Cu-O System

By Ryosuke O. Suzuki*†, Satoshi Okada**, Toshio Oishi* and Katsutoshi Ono*

Electromotive force (*EMF*) measurements using ZrO_2 solid electrolyte were carried out in the Ba-Y-Cu-O system. Gibbs free energies for the reaction in the cell electrodes were summarized in the equations with linear temperature dependency. The standard free energies of the formation of $Y_2Cu_2O_5$ and $YCuO_2$ were derived from *EMF* data and compared with published informations on the stability of $Y_2Cu_2O_5$.

From the results of the X-ray diffraction measurements for the quenched specimens, the phase equilibria in Y-Cu-O system were determined in the temperature range 923 K to 1223 K. Based on the experimental results, $YCuO_2$ was stable above 1115 K and at the oxygen partial pressure higher than 7.18×10^{-4} Pa. In the quaternary Ba-Y-Cu-O system, only a few cell could show the stable *EMF*. The solubilities of barium in both $Y_2Cu_2O_5$ and $YCuO_2$ were negligibly small.

(Received August 16, 1990)

Keywords: *electromotive force, BaY_2CuO_5, $Y_2Cu_2O_5$, $YCuO_2$, free energy, phase diagram*

I. Introduction

$Ba_2YCu_3O_x$ is a well-known oxide superconductor with 90 K class transition temperature (T_c) and considerable efforts have been directed to the practical use. The nonstoichiometry for oxygen of this material is very sensitive to oxygen partial pressure in the annealing atmosphere[1] and it strongly affects the superconductivity. $Ba_2YCu_3O_x$ thin film can be prepared by chemical vapor deposition or sputtering evaporation methods, but few phase diagrams can be utilized at a lower oxygen pressure than $0.21P^\circ$ Pa, (P° Pa = 101325 Pa = 1 atm), because most of the phase diagrams in the BaO-Y_2O_3-CuO system were reported in air for the convenient use[2]-[4]. Both $YCuO_2$[5]-[7] and $BaCu_2O_2$[8] phases were reported to be stable at the lower oxygen pressure and they may form as the by-products in the preparation of $Ba_2YCu_3O_x$[8]. These oxides, however, have rarely been found in the previous phase diagrams of the Ba-Y-Cu-O system.

Electromotive force (*EMF*) method using a zirconia (ZrO_2) solid electrolyte is a powerful technique to measure the oxygen partial pressure (p_{O_2}) of oxides especially in a low pressure region[9]. When *EMF* measurements employing solid electrolyte are made on the following galvanic cell, eq. (1) shows the relationship between *EMF* (E) and temperature (T).

(+) specimen electrode/ZrO_2(+CaO)/reference electrode (−),

$$E = RT/4F \ln (p_{O_2}(\text{specimen electrode}) / p_{O_2}(\text{reference electrode})), \quad (1)$$

where F is the Faraday constant. According to the Gibbs phase rule, p_{O_2} should depend only on the temperature, when three condensed phases in the Y-Cu-O system or four phases in the Ba-Y-Cu-O system are in equilibrium. Under this constraint, the stable *EMF* can be measured as a function of temperature. Several workers have recently reported *EMF* measurements in the BaO-Y_2O_3-Cu_2O-CuO system[6][7][10]-[13] but some early works[10]-[13] have ignored the existence of $YCuO_2$. Wiesner *et al.*[7] have recently showed the free energy change of $YCuO_2$ between 973 and 1273 K by the combination of the gas equilibrium and *EMF* methods.

The purpose of this work is to make clear the phase relationship in the Ba-Y-Cu-O system especially at the oxygen partial pressure lower than $0.21P^\circ$ Pa, and to evaluate the phase stability of $Y_2Cu_2O_5$ and $YCuO_2$. The oxygen potentials in these systems were directly measured by using the solid galvanic cell incorporating the ZrO_2 electrolyte, in reference to the phase relations established experimentally by the present study. The standard free energies of formation, ΔG_f°, for both oxides were derived from *EMF* data as a function of temperature (T) in the temperature range between 953 and 1273 K. Some phase equilibria in the BaO-Y_2O_3-CuO-Cu_2O system were also studied by *EMF* measurements, and their equilibrium p_{O_2} were obtained.

II. Experimental

1. Sample preparation

Powders of the complex oxides in the Ba-Y-Cu-O system were prepared by the normal sintering processes. Stoichiometric amounts of high purity Y_2O_3, CuO and

* Department of Metallurgy, Kyoto University, Yoshida Honmachi, Sakyo-ku, Kyoto 606, Japan.
** Graduate Student, Kyoto University, Kyoto. Present address: Central Research Institute, Mitsubishi Metal Corp., Omiya, Saitama 330, Japan.
† Present address: Nichtmetallische Werkstoffe, ETH-Zentrum, Sonneggstrasse 5, CH-8092, Zürich, Switzerland.

$BaCO_3$ or BaO_2 were mixed in an agate mortar and calcined at 1223 K for 86 ks in open air using the high purity alumina crucible. The calcined samples were pulverized, pressed into pellets and sintered several times at 1223 K in air. The samples were cooled in air after the final sintering at 1273 K. $YCuO_2$ was prepared at 1173 K by reducing $Y_2Cu_2O_5$ under the flow of purified argon gas as reported previously[5].

The sample electrodes of *EMF* measurements were the pellets of the mixture of the oxides. The prepared complex oxides, Y_2O_3, CuO, Cu_2O and/or metallic copper were mixed in a desired composition, compacted into the pellets (8 mm D.A. and 3 mm thick). These pellets were sintered in open air or in the fused silica tube in vacuum. In some cells, they were used without sintering.

2. *EMF* cell constitution and operation

Figure 1 shows a schematic diagram of the *EMF* cell arrangement. The solid electrolyte used in this study was a closed-end ZrO_2+11 mol%CaO tube, 11 mm in I.D., 14 mm in O.D. and 500 mm long. Two electrodes were separated into two rooms by the electrolyte tube to avoid the mutual atmospheric influence of the two electrodes. In order to use air as the reference electrode, a small amount of air was continuously introduced into the bottom of the electrolyte by the air pump, while the purified argon gas was introduced to the sample room. A spiral end of the platinum conducting wire was pushed to the inner bottom of the electrolyte tube using an alumina protection tube. The platinum wire for the sample electrode was put between the electolyte and the sample electrode in order to decrease the electrical resistivity of the measuring cell. When the pellet of the mixture of Ni and NiO powders or the mixture of Cu and Cu_2O powders was used as the reference electrode, they were pushed to the inner bottom of the electrolyte by the alumina tube and the stream of purified argon gas of atmospheric pressure was separately passed over the two half cells.

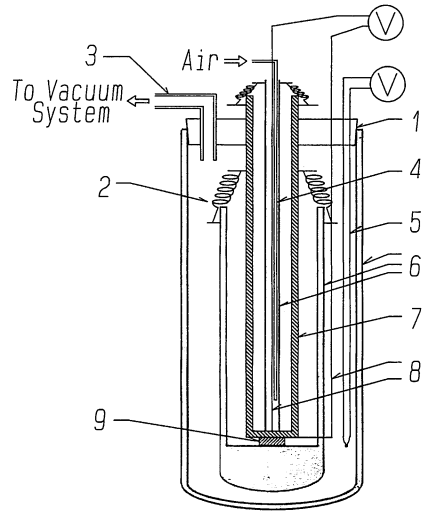

Fig. 1 Schematic cell assembly for *EMF* measurement. 1: Rubber cap, 2: Spring, 3: Copper tube, 4: Stainless steel tube, 5: CA thermocouple, 6: Alumina tubes, 7: ZrO_2 electrolyte tube, 8: Platinum conducting leads.

The temperature was controlled within ±1.0 K during the *EMF* measurements. CA thermocouple was calibrated with the melting points of pure aluminum and silver. The *EMF* of the cell was monitored for both increasing and decreasing temperatures in the range of 923 K and 1273 K with the digital electrometer, which has the input impedance higher than 10^{13} Ω and the reading accuracy of ±0.01 mV. Two or three runs were measured with different molar quantities of oxides for each cell to confirm the reproducibility.

Air(p_{O_2}=0.21$P°$), Ni-NiO equilibrium or Cu-Cu_2O equilibrium was adopted as the standard oxygen partial pressure at the reference electrode in the present study. The latter two p_{O_2} were measured in advance by using air as the reference. p_{O_2} of the Cu_2O-CuO equilibrium was also measured for the calculation afterward. The *EMF* values agreed quite excellently with the previous reports[10][14]-[16]. The following values were used in the present study.

$$\log_{10}(p_{O_2}(\text{Ni-NiO})/P°) = -2.421\times10^4/T+8.676 \quad 923\ \text{K}\le T\le 1273\ \text{K} \tag{2}$$

$$\log_{10}(p_{O_2}(\text{Cu-Cu}_2\text{O})/P°) = -1.705\times10^4/T+7.139 \quad 973\ \text{K}\le T\le 1243\ \text{K} \tag{3}$$

$$\log_{10}(p_{O_2}(\text{Cu}_2\text{O-CuO})/P°) = -1.375\times10^4/T+9.889 \quad 1010\ \text{K}\le T\le 1210\ \text{K} \tag{4}$$

3. Sample characterization

The sintered samples and those after the *EMF* measurements were characterized at room temperature mainly by X-ray diffractometry (Philips PW1700 system) using Cu$K\alpha$ radiation. The results were compared with the JCPDS cards and the previously reported crystallographic data. Electron probe micro-analysis (EPMA, Hitachi X-650) was also done to obtain the compositional profiles. Several specimens were heated in purified helium gas on the platinum heating stage and investigated *in-situ* by X-ray diffractometry.

III. Results

1. Phase relationship in the Y-Cu-O system

When the sample contained yttrium and copper atoms at the molar ratio of one to one, the single phase of $Y_2Cu_2O_5$ was found to be stable in air by X-ray diffraction (XRD) measurements at room temperature. $YCuO_2$[5] was, however, detected in the samples quenched from 1173 K after annealing in the evacuated silica tube. The high pressure phase, $YCuO_3$[17], was not detected in this study.

Figure 2(a) shows the XRD pattern of the single phase of $Y_2Cu_2O_5$ at room temperature. Figure 2 (b) and (c) show the change of XRD patterns of this phase at the elevated temperatures by heating $Y_2Cu_2O_5$ in the purified helium gas. On heating this sample on platinum plate, the lattice parameters of $Y_2Cu_2O_5$ became a little larger,

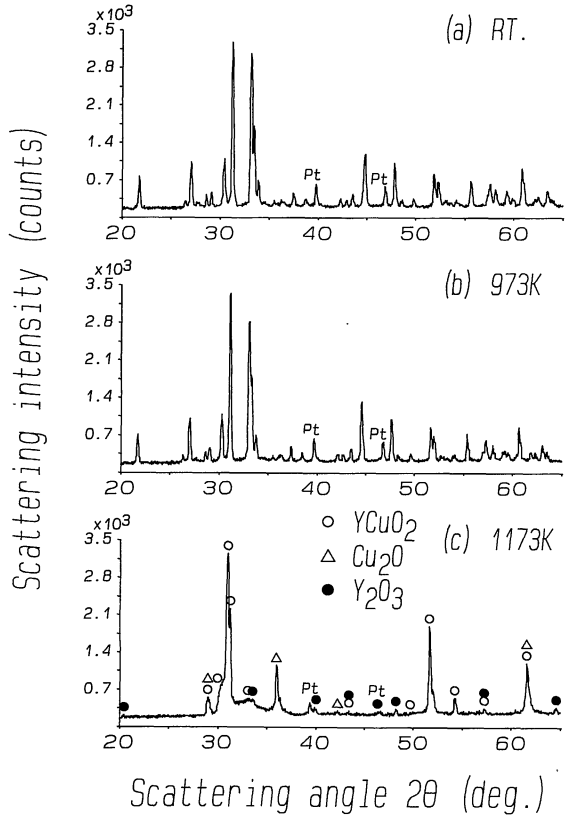

Fig. 2 X-ray diffraction patterns in the sequence of heating $Y_2Cu_2O_5$ on Pt plate in helium gas. The patterns (a) to (c) were measured at room temperature, 973 K and 1173 K, respectively. (a) and (b) were assigned as the single phase of $Y_2Cu_2O_5$.

but $Y_2Cu_2O_5$ was still stable at 973 K. After heating in the purified helium gas from 973 up to 1173 K at the rate of 20 Ks^{-1}, its diffraction was measured *in-situ* at 1173 K after the temperature had stabilized in 0.3 ks. Most of the peaks in Fig. 2(c) were easily assigned by $YCuO_2$ phase[5], and the very weak peaks for Cu_2O and Y_2O_3 were also found. The results of the *in-situ* XRD measurements at the elevated temperatures showed that the phase transformation between $YCuO_2$ and $Y_2Cu_2O_5$ occurred.

The existence of this transformation above 973 K was, therefore, taken into account for the study of phase equilibria. Using the oxide mixture, 18 compositions in the Y_2O_3–Cu–CuO triangle were annealed at 973 K for a week or at 1173 K for 3 d in the evacuated silica tube or in air. Since most of the XRD peaks of $YCuO_2$ coincide with those of $Y_2Cu_2O_5$, Cu_2O, CuO and/or Y_2O_3, the characteristic peak at d=0.16828 nm (54.48°2θ for Cu$K\alpha$) was often used for the identification of $YCuO_2$.

Figure 3 shows the phase relations of oxides in Y–Cu–O ternary system at 1173 K and 973 K. This figure was obtained by summarizing the phase identification of the quenched samples. In Fig. 3, all the phases are illustrated as "stoichiometric compounds" with no solid solubility. Figure 3(a) is well consistent with the recent phase diagrams of Y–Cu–O ternary system[6][7]. According to the literature[5]-[7], $YCuO_2$ is stable at the higher temperature and the lower p_{O_2}. At 973 K, however, $YCuO_2$ could not exist and decomposed into Cu_2O and Y_2O_3. This did not agree with the previous report[7].

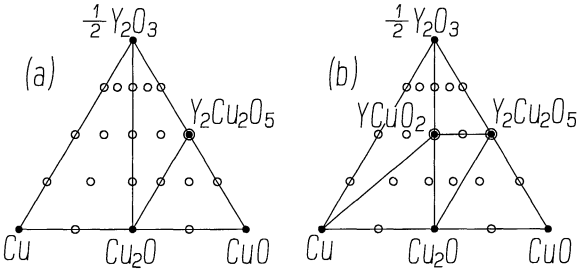

Fig. 3 Phase equilibria in the system Cu–CuO–Y_2O_3 at 973 K (a) and at 1173 K (b). The ○ and ◉ show the experimental compositions.

2. Oxygen potential of the Y–Cu–O system

Based on the phase equilibria in the Y–Cu–O system, *EMF* measurements using ZrO_2 solid electrolyte were carried out on the galvanic cell of the types (I)-(IV) as listed in Table 1. The time required to reach equilibrium varied from 10.8 to 86.4 ks for the cell (I) and from 1.8 to 10.8 ks for the cells (II)-(IV). After these *EMF* measurements, the sample electrodes were confirmed by XRD measurements and EPMA to be the desired phase equilibria. No significant reaction was observed between all the samples and the electrolyte. Table 2 summarizes the observed *EMF*s as a function of temperature. The p_{O_2} at the sample electrodes for these cells were derived by using eqs. (1) and (2), and the results are shown in Fig. 4(a) and (b).

When the solubilities of both Cu_2O and Y_2O_3 in $Y_2Cu_2O_5$ and $YCuO_2$ are negligibly small, the p_{O_2} of both the cells (II) and (III) should be determined by the follow-

Table 1 The construction of the cells measured in this study.

Cell No.	Construction
(I)	Y_2O_3–$Y_2Cu_2O_5$–Cu_2O/ZrO_2/Air
(II)	$Y_2Cu_2O_5$–$YCuO_2$–Cu_2O/ZrO_2/Air
(III)	Y_2O_3–$Y_2Cu_2O_5$–$YCuO_2$/ZrO_2/Air
(IV)	Y_2O_3–$YCuO_2$–Cu/ZrO_2/Ni–NiO
(V)	BaY_2CuO_5–Y_2O_3–$Y_2Cu_2O_5$–Cu_2O/ZrO_2/Air
(VI)	BaY_2CuO_5–Y_2O_3–$Y_2Cu_2O_5$–$YCuO_2$/ZrO_2/Air
(VII)	BaY_2CuO_5–$Y_2Cu_2O_5$–$YCuO_2$–Cu_2O/ZrO_2/Air
(VIII)	BaY_2CuO_5–Y_2O_3–$Y_2Cu_2O_5$–Cu_2O/ZrO_2/Cu–Cu_2O
(IX)	BaY_2CuO_5–Y_2O_3–$Y_2Cu_2O_5$–$YCuO_2$/ZrO_2/Cu–Cu_2O
(X)	BaY_2CuO_5–$Y_2Cu_2O_5$–$YCuO_2$–Cu_2O/ZrO_2/Cu–Cu_2O

Table 2 The observed electromotive forces (*EMF*) for the cell (I) to (X), where e indicates the error at the 95% confidence level for the least squares expression.

Cell	Electromotive force (mV)	e	Temperature (K)
(I)	$-523.4+0.3510\,T$	±0.4	$953 \le T \le 1110$
(II)(III)	$-648.1+0.4629\,T$	±0.4	$1115 \le T \le 1273$
(IV)	$406.5-0.1195\,T$	±0.4	$1160 \le T \le 1260$
(VI)(VII)	$-645.1+0.4601\,T$	±0.4	$1000 \le T \le 1223$
(IX)(X)	$-223.9+0.04651\,T$	±0.4	$1000 \le T \le 1153$

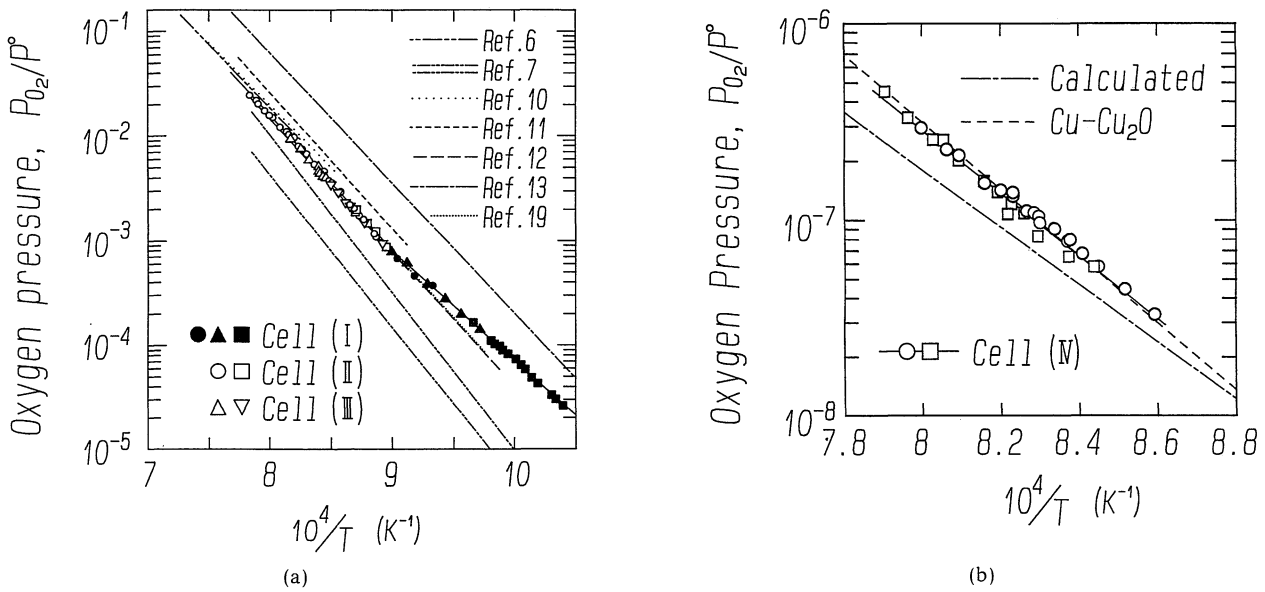

Fig. 4 Oxygen partial pressures in the Y-Cu-O system as a function of the reciprocal absolute temperature, where the solid lines show the linear approximation of this work.

Table 3 Oxygen partial pressures (p_{O_2}) in the Ba-Y-Cu-O system, where, P° and e denote 101325 Pa and the error at the 95% confidence level for the approximation equation of $\log_{10}(p_{O_2}/P^\circ)$, respectively.

Equilibrium	$\log_{10} p_{O_2}/P^\circ$	e	Temperature, T (K)
Y_2O_3-$Y_2Cu_2O_5$-Cu_2O	$6.399-1.055\times10^4/T$	±0.001	$953\leq T\leq1115$
Cu_2O-$Y_2Cu_2O_5$-$YCuO_2$ Y_2O_3-$Y_2Cu_2O_5$-$YCuO_2$	$8.654-1.307\times10^4/T$	±0.001	$1115\leq T\leq1273$
Y_2O_3-$YCuO_2$-Cu	$5.985-1.568\times10^4/T$ $4.886-1.454\times10^4/T$	±0.001 —	$1160\leq T\leq1260$ $1115\leq T\leq1273$*
Cu_2O-$Y_2Cu_2O_5$-$YCuO_2$-BaY_2CuO_5 Y_2O_3-$Y_2Cu_2O_5$-$YCuO_2$-BaY_2CuO_5	$8.664-1.308\times10^4/T$	±0.018	$1000\leq T\leq1223$

* By using the data for cells (I)-(III) and the Cu-Cu_2O equilibrium.

ing equilibrium between $YCuO_2$ and $Y_2Cu_2O_5$:

$$2YCuO_2+1/2O_2=Y_2Cu_2O_5 \quad (5)$$

Because the metal ratio of Y and Cu in $Y_2Cu_2O_5$ (1:1) is the same ratio in $YCuO_2$, the two ternary phase equilibria for cells (II) and (III) should have the same oxygen potential. Wiesner *et al.*[7] reported that there was a small difference between the two potentials because of the non-stoichiometry for $Y_2Cu_2O_5$ and $YCuO_2$. Our experimental results in Fig. 4(a), however, showed that the p_{O_2} of these two cells were quite the same values within the experimental error. Therefore, the temperature dependency of *EMF*s and p_{O_2} for cells (II) and (III) were evaluated into the same equation in Table 3 by using the both data.

By the equations in Table 3, the p_{O_2} for cell (I) and that for cells (II) and (III) have the same value, $8.712\times10^{-4}P^\circ$ Pa, at 1115 K.

3. Oxygen potential of the Ba-Y-Cu-O system

In order to obtain the stable *EMF*s in the Ba-Y-Cu-O system, the measurements were carried out in the coexistence of four condensed phases. When two of the three phases, Cu, Cu_2O and CuO, coexist in the four phases equilibrium, the p_{O_2} of the system is determined by the Cu-Cu_2O or Cu_2O-CuO equilibrium. These kinds of phase equilibria in the Ba-Y-Cu-O system were omitted from the object of the present study. The phase combinations of BaY_2CuO_5-Y_2O_3-$Y_2Cu_2O_5$-Cu_2O, BaY_2CuO_5-Y_2O_3-$Y_2Cu_2O_5$-$YCuO_2$ and BaY_2CuO_5-$Y_2Cu_2O_5$-$YCuO_2$-Cu_2O were found to be stable around the temperature range suitable for *EMF* measurements.

The observed *EMF*s for the cells (V)-(X) are shown in Fig. 5 and Table 2. There was no significant difference for the measured p_{O_2} among the cells (V)-(X). After the *EMF* measurements for the cells (V) and (VIII), however, the X-ray diffractometry for the sample electrodes showed that they were the mixture of 5 phases by the coexistence of a small amount of $YCuO_2$ in addition to the initial phases. The data for these two cells, therefore, were not shown in Table 2. Furthermore, because the data below 1000 K for these cells had the considerable scatter, they were omitted in calculating the least-square approxima-

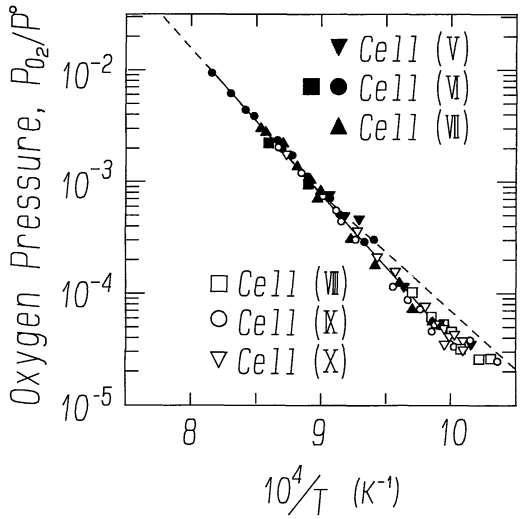

Fig. 5 Oxygen partial pressures in the Ba-Y-Cu-O system as a function of the reciprocal absolute temperature, where the solid line and the broken lines show the linear approximation of this work and that in the Y-Cu-O system of Fig. 4(a), respectively.

tions. The measured p_{O_2} above 1000 K for the 4 cells were, therefore, calculated together as one straight line and are shown in Table 3.

IV. Discussions

1. The standard free energies of $Y_2Cu_2O_5$ and $YCuO_2$

Table 4 shows that the standard free energy changes ($\Delta G°$) for $Cu_2O+Y_2O_3+1/2O_2=Y_2Cu_2O_5$ and for $2YCuO_2+1/2O_2=Y_2Cu_2O_5$. Using these equations, the standard free energies of formation ($\Delta G_f°$) of $Y_2Cu_2O_5$ and $YCuO_2$ from the pure elements were calculated and are shown in Table 5, where the data by Barin *et al.*[14], eqs. (3) and (4) are adopted for calculation of the $\Delta G_f°$ of Y_2O_3, CuO and Cu_2O, respectively.

Table 5 Gibbs free energy of formation ($\Delta G_f°$) from the pure elements (kJ/mol).

Authors	Approximation	at 1000 K	Data used for calculation
for $Y_2Cu_2O_5$			
This work	$-2157+0.4094T$	−1748	$\Delta G_f°(Cu_2O)$, $\Delta G_f°(Y_2O_3)$
Ref. (7)	$-2267+0.4546T$	−1812	$\Delta G_f°(Y_2O_3)$
Ref. (10)	$-2170+0.4231T$	−1747	$\Delta G_f°(Cu_2O)$, $\Delta G_f°(Y_2O_3)$
Ref. (11)	$-2181+0.4325T$	−1748	$\Delta G_f°(Cu_2O)$, $\Delta G_f°(Y_2O_3)$
Ref. (12)	$-2179+0.4286T$	−1750	$\Delta G_f°(CuO)$, $\Delta G_f°(Y_2O_3)$
Ref. (13)	$-2179+0.4288T$	−1750	$\Delta G_f°(CuO)$, $\Delta G_f°(Y_2O_3)$
Ref. (19)	$-2215+0.6861T$ $-0.03135T\ln T$	−1746	—
Authors	Approximation	at 1250 K	Data used for calculation
for $YCuO_2$			
This work	$-1016+0.1633T$	−812.0	$\Delta G_f°(Y_2Cu_2O_5)$*
Ref. (6)	$-1020+0.1665T$	−812.4	$\Delta G_f°(Y_2Cu_2O_5)$*
Ref. (7)	$-1016+0.1788T$	−837.5	$\Delta G_f°(Y_2O_3)$
Ref. (10)**	$-1022+0.1672T$	−812.6	$\Delta G_f°(Y_2Cu_2O_5)$*
Ref. (11)**	$-1016+0.1625T$	−813.3	$\Delta G_f°(Y_2Cu_2O_5)$*
Ref. (12)**	$-1017+0.1645T$	−811.8	$\Delta G_f°(Y_2Cu_2O_5)$*
Ref. (13)**	$-1017+0.1644T$	−811.9	$\Delta G_f°(Y_2Cu_2O_5)$*

* Gibbs free energy of formation of $Y_2Cu_2O_5$ by this work.
** The existence of $YCuO_2$ is supposed.

Supposing that $YCuO_2$ is the stoichiometric compound also for oxygen, the p_{O_2} for the Y_2O_3-$YCuO_2$-Cu equilibrium can be calculated by the data in Table 5. The calculated data marked with an asterisk was also shown in Table 3. The measured p_{O_2} for the cell (IV) shown in Fig. 4(b) was not consistent with that evaluated by $\Delta G_f°$ of $YCuO_2$, but the difference was very small. Since the solubility of yttrium in copper is less than 0.04 at%[18] and that of copper in Y_2O_3 seems to be very small, one can not explain the difference between the calculated p_{O_2} and the measured one.

The measured values agreed better with that of Cu-

Table 4 Standard free energy change of the reaction, $\Delta G°$ (kJ/mol).

	$Cu_2O+Y_2O_3+1/2O_2=Y_2Cu_2O_5$				
References	Approximation	Error	Temperature range	at 973 K	at 1073 K
This work	$-101.0+0.06126T$	±0.069	$953\leq T\leq 1110$ K	−41.39	−35.27
Ref. (7)	$-151.1+0.09822T$	—	$973\leq T\leq 1273$	−55.50	−45.68
Ref. (10)	$-110.9+0.07189T$	±0.16	$1173\leq T\leq 1340$	−40.95	−33.76
Ref. (11)	$-124.3+0.08433T$	±0.21	$1097\leq T\leq 1292$	−42.29	−33.85
Ref. (12)	$-122.5+0.08046T$	—	$1013\leq T\leq 1273$	−44.22	−36.18
Ref. (13)	$-122.5+0.08066T$	±1.00	$1025\leq T\leq 1220$	−44.04	−35.97
Ref. (19)	$-132.5+0.09822T-0.0118T\ln T$	—	—	−37.60	−29.08
	$2YCuO_2+1/2O_2=Y_2Cu_2O_5$				
References	Approximation	Error	Temperature range	at 973 K	at 1073 K
This work	$-125.1+0.08285T$	±0.068	$1115\leq T\leq 1273$ K	−27.92	−19.63
Ref. (6)	$-116.295+0.0765T$	—	$1213\leq T\leq 1375$	−26.56	−18.91
Ref. (7)*	$-144.956+0.096963T$	—	$973\leq T\leq 1273$	−31.22	−21.52
Ref. (7)**	$-140.483+0.089750T$	—	$973\leq T\leq 1273$	−35.21	−26.23

* Reported value based on the Y_2O_3-$YCuO_2$-$Y_2Cu_2O_5$.
** Reported value based on the Cu_2O-$YCuO_2$-$Y_2Cu_2O_5$.

Cu_2O. This may be due to the contamination of the sample electrode by Cu_2O. One of the reasons for the appearance of Cu_2O is that a part of $YCuO_2$ in the sample electrodes might have decomposed into Cu_2O and Y_2O_3 during heating from room temperature. The another possibility is that initial $YCuO_2$ might have contained a small amount of Cu_2O. However, X-ray diffractometry and EPMA could not detect clearly the existence of Cu_2O in the samples after *EMF* measurements.

In this work, therefore, the data of cell (IV) were not used for further discussions, and ΔG_f° of $YCuO_2$ in Table 5 was deduced by the cell (I)-(III) and ΔG_f° of Cu_2O.

2. Comparisons with previous studies

In Fig. 4(a) the previous studies are also shown for comparison. Tretyakov *et al.*[10], Pankajavalli *et al.*[11], Borowiec *et al.*[12] and Simpo *et al.*[13] measured the p_{O_2} for Cu_2O-Y_2O_3-$Y_2Cu_2O_5$ by using the ZrO_2 solid electrolyte. On the other hand, Zhang *et al.*[6] and Wiesner *et al.*[7] studied the p_{O_2} for Cu_2O-$YCuO_2$-$Y_2Cu_2O_5$ and Y_2O_3-$YCuO_2$-$Y_2Cu_2O_5$ using the combination of the thermogravimetry and the gas equilibrium method. Lee *et al.*[19] calculated the free energy changes based on the phase diagrams in air. The p_{O_2} for Cu_2O-Y_2O_3-$Y_2Cu_2O_5$ reported by *EMF* methods[10]-[13] are well consistent with those for Cu_2O-$Y_2Cu_2O_5$-$YCuO_2$ and Y_2O_3-$Y_2Cu_2O_5$-$YCuO_2$ by this work. It should be noted that the early workers[10]-[13] did not notice the existence of $YCuO_2$ at the higher temperature. The p_{O_2} for $Y_2Cu_2O_5$-$YCuO_2$ reported by Zhang *et al.*[6] also agreed well with that of the present study. The p_{O_2} by Wiesner[7] showed a little difference from that by this study. Since the reported data were obtained by the gas equilibrium method, there may be a doubt whether or not the equilibrium between the samples and the atmospheric oxygen was achieved especially at the lower p_{O_2} and lower temperatures. The *EMF* method, however, has the advantage that it can directly detect the p_{O_2} of the sample electrodes even under such experimental conditions.

The thermodynamic data were also evaluated from the reported data by using the standard free energies of formation of Y_2O_3[14] and copper oxides. In Tables 4, the ΔG° for the two reactions are compared with the other reports[6][7][10]-[13][19]. Table 5 shows the ΔG_f° of $Y_2Cu_2O_5$ and $YCuO_2$ in the literature[6][7][10]-[13][19] for the comparison. The ΔG_f° of $YCuO_2$ were recalculated from their values for '$Y_2Cu_2O_5$', supposing the existence of $YCuO_2$ above 1115 K. The standard free energy change of formation of $Y_2Cu_2O_5$ in this work is well consistent with the previous works below 1115 K. The reported data and the re-evaluation for $YCuO_2$ agreed very well with the present work for $YCuO_2$ within the difference of 2 kJ/mol at 1250 K.

3. Relations between oxygen potential and stable phases

By assessing the data in Table 3, Fig. 6(a) and Fig. 6(b) show the p_{O_2} at 1000 and 1250 K as a function of metallic ratio of Cu/Y. These calculated potential diagrams are

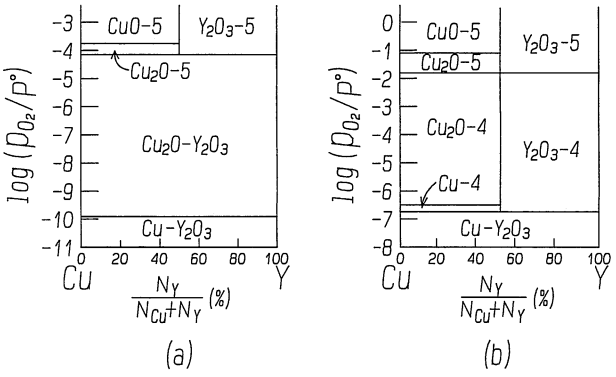

Fig. 6 Oxygen partial pressures as a function of metallic ratio of Y and Cu at 1000 K (a) and at 1250 K (b), where $Y_2Cu_2O_5$ and $YCuO_2$ are referred to as "*5*" and "*4*", respectively.

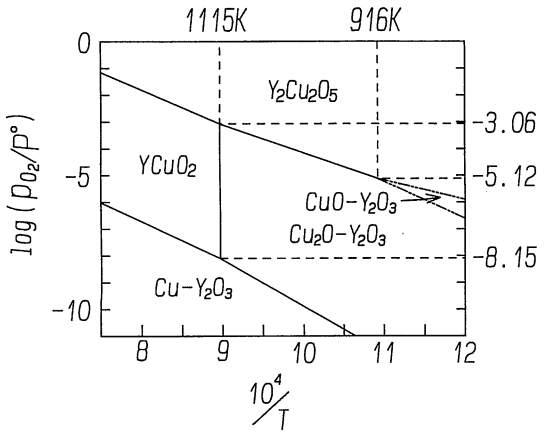

Fig. 7 Oxygen partial pressure of $Y_2Cu_2O_5$ and $YCuO_2$ at the metallic ratio of Y/Cu=1.

consistent with the experimental phase diagrams in Fig. 3. Figure 7 shows the stable region of $YCuO_2$ single phase at the composition of Cu/Y=1.

Figures 6 and 7 show there are at least 2 invariant reactions; (1) Y_2O_3-$YCuO_2$-$Y_2Cu_2O_5$-Cu_2O at 1115 K and at $p_{O_2}/P^\circ = 8.712 \times 10^{-4}$, and (2) Y_2O_3-$YCuO_2$-Cu_2O-Cu at 1115 K and at $p_{O_2}/P^\circ = 7.087 \times 10^{-9}$. By extrapolating to the lower temperature, the equilibrium of Y_2O_3-$Y_2Cu_2O_5$-CuO-Cu_2O might exist at 916 K and at $p_{O_2}/P^\circ = 7.50 \times 10^{-6}$. This suggests that $Y_2Cu_2O_5$ decomposes directly into Y_2O_3 and CuO below 916 K.

The oxygen potential of cells (VI), (VII), (IX) and (X) in the Ba-Y-Cu-O system agreed quite well with that of cells (II) and (III) in the Y-Cu-O system. This shows that the activities of $Y_2Cu_2O_5$ and $YCuO_2$ are not affected by the addition of barium: there are no appreciable solubility of barium in these oxides. Even below 1115 K, however, the decomposition of $YCuO_2$ into Cu_2O and Y_2O_3 in the four phase equilibria including BaY_2CuO_5 was not observed in *EMF* measurements and X-ray diffractometry for the annealed specimens. The stabilization of $YCuO_2$ may be caused by adding barium.

V. Conclusion

The relation between oxygen potential and the stable phases was shown on the basis of experimental results. $Y_2Cu_2O_5$ was found to decompose into $YCuO_2$ above 1115 K. The 10 kinds of electromotive force measurements were carried out using ZrO_2 solid electrolyte in the Ba-Y-Cu-O system. From the observed *EMF*s, the p_{O_2} in Ba-Y-Cu-O system and the related thermodynamical values of $Y_2Cu_2O_5$ and $YCuO_2$ were derived at the temperature range between 953 K and 1273 K. These results are in good agreement with the other investigators, supposing the existence of $YCuO_2$ in their reports. Since the measured oxygen potential for Cu_2O-$YCuO_2$-$Y_2Cu_2O_5$-BaY_2CuO_5 agreed well with that for Cu_2O-$YCuO_2$-$Y_2Cu_2O_5$, barium does not change the activity of $YCuO_2$ nor $Y_2Cu_2O_5$.

Acknowledgments

The authors thank Prof. K. Osamura, Mr. W. Zhang in Kyoto University and Dr. I. Katayama in Osaka University for their valuable discussions, Mr. K. Kimura, Mr. I. Nakagawa, Mr. T. Unezaki and Mr. M. Hamura for their invaluable experimental assistance, and Mr. K. Sasaki and Mr. H. Murakami for performance of a part of the *EMF* measurements. This work was financially supported in part by the KURATA foundation and by the Grant-in-Aid for Encouragement of Young Scientists through the Ministry of Education, Science and Culture, Japan.

REFERENCES

(1) D. R. Clarke, T. M. Shaw and D. Dimos: J. Am. Ceram. Soc., **72** (1989), 1103.
(2) K. G. Frase and D. R. Clarke: Adv. Ceram. Mater., **2**, Spec. Iss. (1987), 295.
(3) R. S. Roth, K. L. Davis and J. R. Dennis: Adv. Ceram. Mater., **2**, Spec. Iss. (1987), 303.
(4) K. Osamura, W. Zhang, T. Yamashita, S. Ochiai and B. Predel: Z. Metallk., **79** (1988), 693.
(5) T. Ishiguro, N. Ishizawa, N. Mizutani and M. Kato: J. Sol. Stat. Chem., **49** (1983), 232.
(6) W. Zhang and K. Osamura: Z. Metallk., **81** (1990), 196. Their values of the standard free energy in their report are halved according to their experimental results.
(7) U. Wiesner, G. Krabbes and M. Ritschel: Mat. Res. Bull., **24** (1989), 1261.
(8) B. T. Ahn, V. Y. Lee, R. Beyers, T. M. Gür and R. A. Huggins: Physica **C167** (1990) 529.
(9) E. C. Subbarao: *Solid Electrolytes and Their Applications*, Plenum Press, New York, (1980).
(10) Yu. D. Tretyakov, A. R. Kaul and N. V. Makukhin: J. Sol. Stat. Chem., **17** (1976), 183.
(11) R. Pankajavalli and O. M. Sreedharan: J. Mater. Sci. Lett., **7** (1988), 714.
(12) K. Borowiec and K. Kolbrecka: Jpn. J. Appl. Phys., **28** (1989), L1963.
(13) R. Simpo and Y. Nakamura: J. Japan Inst. Metals, **54** (1990), 549.
(14) I. Barin and O. Knacke: *Thermochemical properties of inorganic substances*, Springer-Verlag, Berlin, (1973), and I. Barin, O. Knacke and O. Kubaschewski: *Thermochemical properties of inorganic substances, Supplement*, Springer-Verlag, Berlin, (1977).
(15) K. Kiukkola and C. Wagner: J. Electrochem. Soc., **104** (1957), 379.
(16) O. Kubaschewski and C. B. Alcock: *Metallurgical Thermochemistry*, 5th ed., Pergamon Press, Oxford, (1983).
(17) M. Arjomand and D. J. Machin: J. Chem. Soc., Dalton Trans., **II** (1975), 1061.
(18) D. J. Chakrabarti and D. E. Laughlin: Bull. Alloy Phase Diagram, **2** (1981), 315.
(19) B.-J. Lee and D. N. Lee: J. Am. Ceram. Soc., **72** (1989), 314.